An Unexpected Crystal-Chemical Principle for the Pyrochlore Structure

Terrell A. Vanderah,*[a] Igor Levin,[a] and Michael W. Lufaso[a]

Keywords: Pyrochlore / Displacive disorder / Bismuth zinc niobates / Phase equilibria

Phase equilibrium studies of the Bi–Zn–Nb–O system show that pyrochlore does not form at chemical compositions predicted by the traditional formula for this crystal structure, $A_2B_2O_6O'$, where A denotes large (8-coordinated, e.g. Bi^{3+}) and B small (6-coordinated, e.g. Zn^{2+}, Nb^{5+}) cation sites. Instead, pyrochlore forms only at compositions with excess B cations which, surprisingly, occupy the large A-cation sites. Reports of similar behavior in other pyrochlores suggest a previously unrecognized inherent structural feature (displacive disorder) which allows the formation of a large family of cubic pyrochlores with small B cations occupying up to ca. 25 % of the large A-cation sites. Many pyrochlores can now be synthesized by deliberately combining large and small metal ions on the A sites.

Introduction

The mineral pyrochlore, $(Na,Ca)_2Nb_2O_6(OH,F)$, was named in 1826 from the Greek for *fire* and *green* because some specimens turned green upon ignition.[1] *Pyrochlore* also denotes a large group of 22 crystallographically similar minerals that are highly diverse chemically[2] and widely distributed geologically. The general formula is $\mathbf{A_{1\rightarrow2}B_2O_6(O,OH,F)\cdot}\boldsymbol{n}\mathbf{H_2O}$, where, in geological specimens, **A** is a relatively large cation (Ca, K, Ba, Y, Ce, Pb, U, Sr, Cs, Na, Sb^{3+}, Bi, and/or Th; radii larger than or equal to ca. 1.0 Å) and **B** is a smaller cation (Nb, Ta, Ti, Sn, Fe, and/or W); the seventh anion position in the crystal structure can be occupied by O^{2-}, OH^-, and/or F^-.[1]

A large number of pyrochlore analogs have been synthesized with an amazing variety of chemical compositions and exploitable properties.[3–9] These include ferroelectricity,[4,10,11] temperature-stable high-permittivity properties,[12,13] fast-ion oxygen conductivity,[6–8] and a wide variety of electrical properties including metallic conductivity, semiconductivity, superconductivity, and electronic phase transitions.[4,5,14–18] The threefold symmetry of the metal arrangement in the crystal structure leads to interesting and diverse magnetic-ordering properties such as ferromagnetism, antiferromagnetism, and spin-glass behavior;[19–21] colossal magnetoresistance (CMR) has also been observed.[22,23] Pyrochlores are known to exhibit catalytic properties,[6] optical properties of interest for pigments and luminescent materials,[6,24] and refractory properties resulting in their consideration as host ceramics for nuclear waste immobilization.[4,25]

The remarkable variety of properties obtainable with the pyrochlore crystal structure reflects its inherent chemical and structural versatility. This non-molecular arrangement[4,5,26,27] is unusual in that it can be considered as two relatively independent, interpenetrating three-dimensional frameworks (Figure 1). The $A_2B_2O_7$ overall formula for ideal oxide pyrochlores is often written as $A_2B_2O_6O'$ (or $A_2B_2O_6X$) to distinguish the oxygen atoms (or anions) in the two different networks. The ideal cubic structure is highly symmetrical, crystallizing in space group $Fd\bar{3}m$ (No. 227), with four crystallographically distinct sites occupied by the A (site 16*d*), B (site 16*c*), O (site 48*f*), and O′ (site 8*b*) ions. Symmetry fixes the positions of all ions except those in 48*f*, which have a single variable parameter along the *x*-direction. The extensive compositional ranges known for pyrochlore compounds reflect the versatility of the A_2O' substructure: "defect" pyrochlores form readily since this network can be partially occupied or even completely absent, as in the pyrochlore-type polymorph of WO_3 (W_2O_6).[29] In addition, the O′ position can be occupied by anions other than O^{2-} such as OH^-, F^-,[30] and S^{2-},[31] forming oxyhydroxide, oxyfluoride, and oxysulfide pyrochlores. A number of non-oxide pyrochlores are known[27,32] including chlorides[33] and fluorides.[34,35] The pyrochlore structure is therefore highly "tailorable"; e.g., the identities and oxidation states of the B-cations, which play a leading role in electronic properties, can be controlled by achieving electroneutrality through deliberate choices of the A and O′ ions and their concentrations.

Although solid-state chemists realize that ions are not hard spheres with fixed sizes, the use of *structure field maps*[36] to predict the crystalline arrangement of new complex oxides has been moderately successful, especially given the scarcity of theoretical tools. For a given crystal structure, the map is constructed empirically from known com-

[a] National Institute of Standards and Technology, Ceramics Division,
Gaithersburg, MD 20899, USA

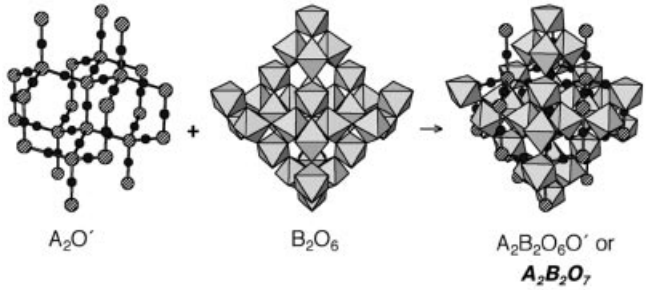

Figure 1. The ideal crystal structure of pyrochlore represented as two interpenetrating networks. Small black spheres denote A cations, large hatched spheres represent O′ oxygen anions, and gray octahedra contain B cations with oxygen atoms located at the six vertices. The A_2O' network corresponds to that of anticristobalite-type[28] Cu_2O, featuring four-coordinate O′ ions and two-coordinate A cations. The B_2O_6 framework consists of $[BO_6]$ octahedra sharing all vertices to form large cavities. The structures are interwoven such that the O′ ions of the A_2O' network occupy the centers of these cavities, while the A cations reside in puckered hexagons formed by oxygen atoms in the B_2O_6 framework. The final coordination number of the A cations is eight including the two oxygen atoms in the A_2O' network, which cap the puckered hexagonal ring above and below.

pounds by plotting the ionic radii[37] of the A vs. the B cations; new compounds may form the same structure if the radii of the proposed A and B cations correspond to a point in the observed stability field. The use of structure field maps and cation radius ratios to predict the formation of pyrochlores has been somewhat successful for ideal formulations.[4,8,38–41] For example, for $A^{3+}{}_2B^{4+}{}_2O_7$ pyrochlores, the A cation can be as small as Lu^{3+} (0.977 Å) or as large as Bi^{3+} (1.17 Å), while the radii of the B cations fall between ca. 0.58 and 0.72 Å.[4] The approach has been less useful for pyrochlores with substitutions on the A and B sites;[6,42] nevertheless, there is general agreement that the A cation must be appreciably larger than the B cation for the structure to form.

In the late 1990s, pyrochlore-containing Bi–Zn–Nb–O materials attracted considerable attention as they were found to exhibit properties suitable for embedded (miniaturized) temperature-stable capacitors and filters.[12,43] The composition of the pyrochlore phase was given in numerous reports as $Bi_{1.5}Zn_{1.0}Nb_{1.5}O_7$, which incited considerable controversy since this would require half of the small Zn^{2+} cations (radius 0.74 Å) to be mixed with the much larger Bi^{3+} ions on the A sites of the structure [i.e., $Bi_{1.5}Zn_{0.5}(Zn_{0.5}Nb_{1.5})O_7$, B-site cations in parentheses]. The size of Zn^{2+}, which is rarely observed with coordination numbers higher than 6, falls well outside the structure field maps for the A site cations in ideal pyrochlores.[4,40] Subsequently, the composition $Bi_{1.5}Zn_{1.0}Nb_{1.5}O_7$ was shown to be a two-phase mixture of pyrochlore and ZnO; however, a pure single-phase cubic pyrochlore was indeed obtained at the composition $Bi_{1.5}Zn_{0.92}Nb_{1.5}O_{6.92}$,[44] which also requires a considerable concentration of Zn^{2+} on the A sites.

A structural determination of $Bi_{1.5}Zn_{0.92}Nb_{1.5}O_{6.92}$[44] revealed static displacive disorder in the A_2O' portion of the structure and concluded a structural formula of $Bi_{1.5}Zn_{0.42}\square_{0.08}(Zn_{0.50}Nb_{1.5})O_{6.92}$. The A sites were assumed to be occupied by a (disordered) mixture of Bi^{3+}, Zn^{2+}, and vacancies (□); observation of reflections with Miller indices 442, forbidden for an ideal pyrochlore, required lower-symmetry positions for the A and O′ ions, even though the average structure retains cubic symmetry [$Fd\bar{3}m$, a = 10.5616(1) Å] The combined displacements (Figure 2) of the A (0.39 Å) and O′ (0.46 Å) ions change the coordination number of the A cations from 8 to (5 + 3), thus permitting the smaller Zn^{2+} ion to achieve a chemically reasonable environment, with fewer nearest oxygen neighbors, by local correlations of the displaced ions, as

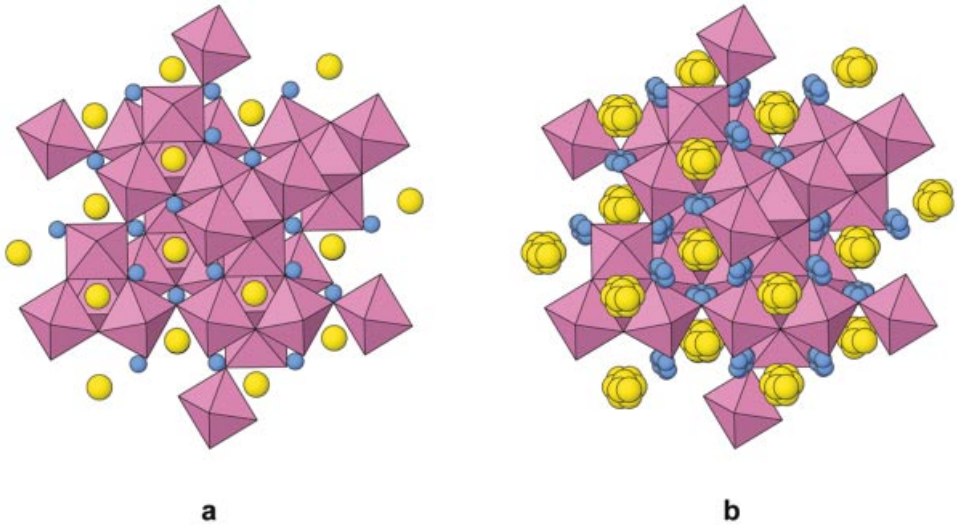

Figure 2. Comparison of the ideal (**a**) pyrochlore structure (Figure 1) and actual (**b**) structure determined for $Bi_{1.5}Zn_{0.92}Nb_{1.5}O_{6.92}$, with displacive disorder in the A_2O' network.[44] Blue spheres represent A cation sites, yellow spheres represent the O′ oxygen sites (bonds in the A_2O' network have been omitted for clarity), and red octahedra denote the B_2O_6 framework. In part **b**, a disordered mixture of Bi^{3+}, Zn^{2+}, and vacancies is distributed randomly among the six equivalent sites represented by each toroid of blue spheres; cuboctahedral clusters of yellow spheres denote the 12 possible displaced positions for the O′ ions.

subsequently confirmed by a detailed study of diffuse scattering.[45] Single-crystal X-ray diffraction analysis[46] also confirmed the displacively disordered structural model for $Bi_{1.5}Zn_{0.92}Nb_{1.5}O_{6.92}$. Interestingly, vibrational spectroscopic studies suggest that the glass-like dielectric behavior observed for $Bi_{1.5}Zn_{0.92}Nb_{1.5}O_{6.92}$ is caused by this displacive disorder.[44,47] The present study of the equilibrium phase diagram for the Bi_2O_3–ZnO–Nb_2O_5 system was carried out to elucidate the compositional range of this highly unusual pyrochlore as well as its thermodynamic compatibility with other phases in the system.

Results and Discussion

Subsolidus phase relations obtained for the Bi_2O_3–ZnO–Nb_2O_5 system are shown in Figure 3. The previously reported binary phase equilibria for the perimeter systems (Bi_2O_3–Nb_2O_5,[48–50] Bi_2O_3–ZnO,[51] ZnO–Nb_2O_5[52,53]) were confirmed in the present study, with the exception of the Bi_2O_3–Nb_2O_5 system above 0.75 Bi_2O_3 (represented here as a solid solution extending to Bi_2O_3) which we did not investigate in detail. This region apparently forms a series of modulated fluorite superstructures;[49] differences in the reported diagrams likely arise from variations in cooling methods and whether specimens were examined by X-ray or electron diffraction methods.

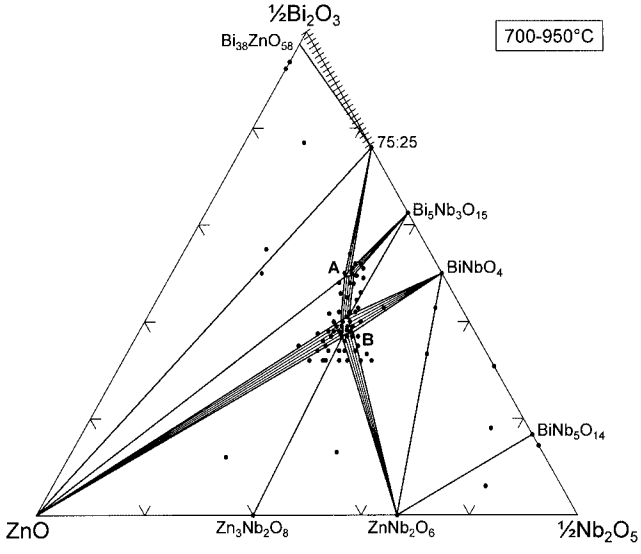

Figure 3. Subsolidus phase equilibrium diagram in air for the Bi_2O_3–ZnO–Nb_2O_5 system. Black dots denote the compositions of specimens prepared in the study; concentrations are on a molar fraction basis. Ternary phase formation is limited to zirconolite (A) and pyrochlore (B), both of which form single-phase solid solution regions. As shown, zirconolite forms thermodynamically stable mixtures with pyrochlore, ZnO, the 75:25 Bi_2O_3:Nb_2O_5 solid solution, and $Bi_5Nb_3O_{15}$. Bi–Zn–Nb–O pyrochlores will form stable mixtures with zirconolite, $Bi_5Nb_3O_{15}$, $BiNbO_4$, $ZnNb_2O_6$, $Zn_3Nb_2O_8$, and ZnO. Temperature-stable dielectric ceramics are processed in the two-phase region indicated between zirconolite (A) and pyrochlore (B).

Only two ternary phases were found to form in the Bi_2O_3–ZnO–Nb_2O_5 system, monoclinic zirconolite[54,55] (A) and cubic pyrochlore (B) (Figure 3). Observable shifts in their X-ray powder diffraction patterns indicated that both compounds are nonstoichiometric and form solid solution regions. Pyrochlore does not form at the conventionally predicted composition $Bi_2Zn_{2/3}Nb_{4/3}O_7$, which falls in the zirconolite region A. Instead, pyrochlore forms at substantially lower Bi concentrations in this chemical system. The present results indicate, in fact, that the single-phase field for the pyrochlore structure falls *completely outside* compositions predicted for conventional pyrochlores, i.e., those with Bi^{3+} on the A sites and a Zn^{2+}/Nb^{5+} mixture on the B sites, as shown in Figure 4. We conclude that the unconventional placement of small B-type cations such as Zn^{2+} on the large A-cation sites, accompanied by displacive disorder in the A_2O' network, is *required* for stabilization of the pyrochlore structure in the Bi–Zn–Nb–O system.

A number of reports found in the literature suggest that displacive disorder in the A_2O' network is an inherent feature of the pyrochlore structure. Nearly thirty years ago, a detailed structural study of $Sn^{2+}{}_{1.76}(Ta_{1.56}Sn^{4+}{}_{0.44})O_{6.54}$[56] found that Sn^{2+} was displaced 0.38 Å from the ideal A-cation positions, nearly the same as in $Bi_{1.5}Zn_{0.92}Nb_{1.5}O_{6.92}$. These authors mention observation of the "forbidden" 442 reflection as "glaring" evidence of deviation from the ideal pyrochlore structure. Similar behavior was found for $Bi_{1.74}Ti_2O_{6.62}$, again with Bi^{3+} displacements of 0.38 Å,[57] and also for the stoichiometric compound $Bi_2Ti_2O_7$.[58] Pyrochlore-type $Tl_2Nb_2O_{6+x}$ compounds were also found to exhibit Tl ion displacements, apparently dynamic at room temperature.[59] Numerous titanate and zirconate pyrochlores with rare earth A-cations are known to exhibit characteristic diffuse intensity distributions[60] analogous to those observed for β-cristobalite (SiO_2), which features atoms in the same positions as the A_2O' network of pyrochlore. A study of $La_2Zr_2O_7$ concluded that the La^{3+} ions do not occupy the ideal A sites, but are dynamically disordered around an annulus perpendicular to the O′–La–O′ linear unit.[60] This behavior is analogous to the orientational disorder of the [SiO_4] tetrahedra in β-cristobalite, which results in typical Si–O bond lengths and angles as opposed to the chemically unreasonable values in the average structure. Similar improvements in bond lengths are achieved for La^{3+} in the pyrochlore $La_2Zr_2O_7$ by this mechanism;[60] the annulus containing the La positions occurs in the same plane as the toroids of six possible A sites in $Bi_{1.5}Zn_{0.92}Nb_{1.5}O_{6.92}$ (Figure 2, part b).

The unconventional substitution of small B-type cations on the A sites of pyrochlore has also been previously observed; the present results as well as several other reports suggest that up to about 25% of the A sites in the $A_2B_2O_6O'$ structure can be substituted with small, typically B-site cations. Examples include the ferroelectric oxysulfide pyrochlore $Cd_{2-x}Zn_xNb_2O_6S$,[31] and the series $Bi_{2-x}B_xRu_2O_{7-y}$ (B = Mn, Co, Ni, Cu, Zn, Mg), with x-values as high as 0.5.[16] Similar cubic pyrochlores have been reported with Nb instead of Ru; i.e., $Bi_{1.5}MNb_{1.5}O_7$ (M = Cu, Mg, Mn, Ni), which would require half of the small M cations to be mixed with Bi^{3+} on the A sites.[61] These re-

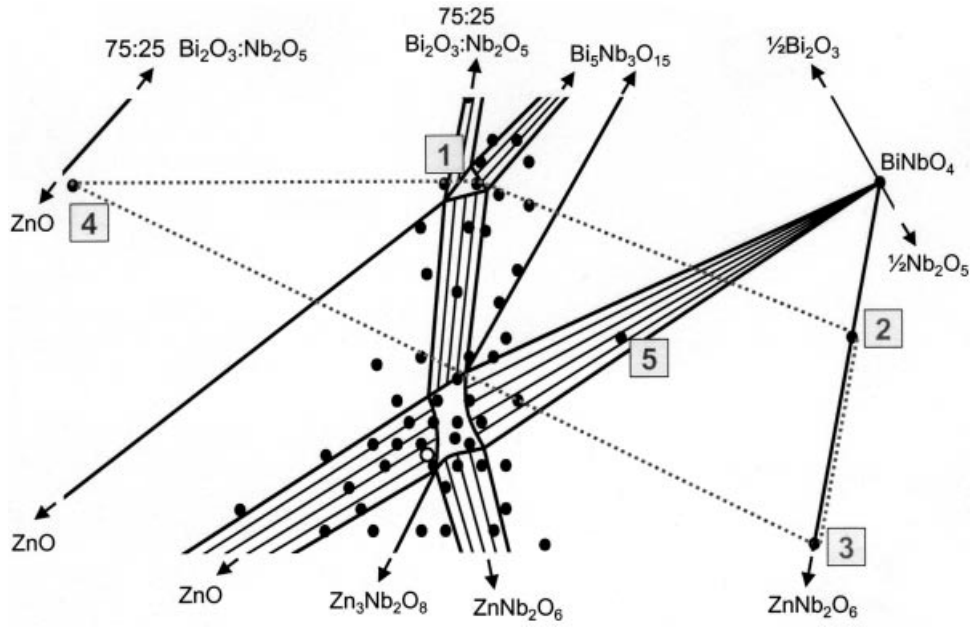

Figure 4. Magnified portion of the Bi_2O_3–ZnO–Nb_2O_5 phase equilibrium diagram (Figure 3), emphasizing the regions of zirconolite and pyrochlore phase formation. The zirconolite structure forms at compositions within the small triangle containing the composition $Bi_2Zn_{2/3}Nb_{4/3}O_7$ (1). The cubic pyrochlore phase forms within the four-sided region below zirconolite. Joins (lines) emanate from the curved sides and vertices of this region to compounds that form thermodynamically stable two-phase mixtures with pyrochlore. The dotted line connects compositions 1 ($Bi_2Zn_{2/3}Nb_{4/3}O_7$), 2 ($Bi_{1.5}Zn_{0.166}Nb_{1.833}O_7$), 3 ($BiZn_{1/3}Nb_{5/3}O_6$), and 4 ($Bi_2Zn_{4/3}Nb_{2/3}O_6$) to outline the compositional field in which conventional pyrochlores and/or defect pyrochlores are expected to form (5 = $Bi_{1.5}Zn_{0.5}Nb_{1.5}O_{6.5}$); i.e., with no Zn^{2+} ions on the A sites. The single-phase region found for pyrochlore is seen to fall *completely outside* this field, indicating that the structure only forms at compositions with excess B cations that are accommodated on A sites. The open circle in the two-phase ZnO-pyrochlore field corresponds to the composition $Bi_{1.5}Zn_{1.0}Nb_{1.5}O_7$, given in numerous reports as the stoichiometry of the pyrochlore phase, but which actually lies outside the single-phase region.

ports do not include detailed X-ray powder diffraction data; however, all of these cubic pyrochlores should exhibit displacive disorder in the A_2O' network to provide chemical accommodation of the small B-type cations – their X-ray powder diffraction patterns should exhibit weak forbidden reflections such as the 442, which can be indexed using the reported $Fd\bar{3}m$ cubic unit cells, but which serve as (easily overlooked) diagnostic flags for the displacement of atoms to lower-symmetry positions in the space group.

The present study confirmed observation of weak peaks at the positions of the diagnostic 442 reflections in the powder diffraction patterns for pyrochlore phases forming in the systems Bi–M–Nb–O with M = Co, Fe, Ni, Mn, Cu, and Cr, as shown in Figure 5. As in the Bi–Zn–Nb–O system, the pyrochlore phase in these systems does *not* form as a pure compound at conventional formulations (i.e. $Bi_2Co_{2/3}Nb_{4/3}O_7$, $Bi_2Ni_{2/3}Nb_{4/3}O_7$, Bi_2FeNbO_7, Bi_2MnNbO_7, $Bi_2Cu_{2/3}Nb_{4/3}O_7$, or Bi_2CrNbO_7). Recent phase equilibrium studies of the Bi_2O_3–Mn_2O_3–Nb_2O_5 and Bi_2O_3–Fe_2O_3–Nb_2O_5 systems[62] found that, similar to the Bi_2O_3–ZnO–Nb_2O_5 system (Figure 3), the pyrochlore single-phase fields occur at substantially lower Bi concentrations than the conventional formulas, and at compositions requiring the mixing of B-type Mn and Fe cations on the A-sites with Bi^{3+}. Furthermore, *all* X-ray powder diffraction patterns for pyrochlore and pyrochlore-containing specimens in these studies exhibited clearly observable 442 reflections. We conclude that, as for the Bi–Zn–Nb–O system, the occurrence of displacive disorder in the A_2O' network is *required* for the formation of pyrochlore in the Bi–Mn–Nb–O and Bi–Fe–Nb–O chemical systems. We refer to these as misplaced-displacive cubic pyrochlores – pyrochlores which exhibit misplacement of traditionally octahedral B-site cations onto the larger A-sites, accompanied by displacive disorder in the A_2O' substructure to facilitate lower coordination numbers for the smaller species.

A structural study of the cubic pyrochlores $Bi_2Ru_2O_7$, $Bi_{1.6}Cu_{0.4}Ru_2O_7$, and $Bi_{1.6}Co_{0.4}Ru_2O_7$[14] confirmed static displacive disorder in both the A and O′ sites for all three compounds, and proposed that this was a common feature of $A_2B_2O_7$ pyrochlores having a lone electronic pair on the A-site cation (e.g. Bi^{3+}, Pb^{2+}, Tl^+). Similar conclusions were drawn for the series $Bi_{2-y}Yb_yRu_2O_{7-\delta}$[18] and $Bi_{2-x}(CrTa)O_{7-y}$[63] More generally, we suggest that this is an inherent feature of the chemically versatile pyrochlore structure which occurs to accommodate cations with shapes (i.e. lone pairs) or sizes (i.e. typical B-type cations) that are non-ideal for the coordination environment provided by the rigid B_2O_6 framework. This more general principle is demonstrated in the Ca-Ti–Nb–O system, which forms a cubic pyrochlore near the composition $Ca_{1.5}Ti_{1.5}NbO_7$ [=$Ca_{1.5}Ti_{0.5}(TiNb)O_7$].[64] Structural studies of single crystals of $Ca_{1.5}Ti_{1.5}NbO_7$ and also isostructural $Ca_{1.5}Ti_{1.5}TaO_7$[65] revealed displacive disorder in both the A and O′ positions

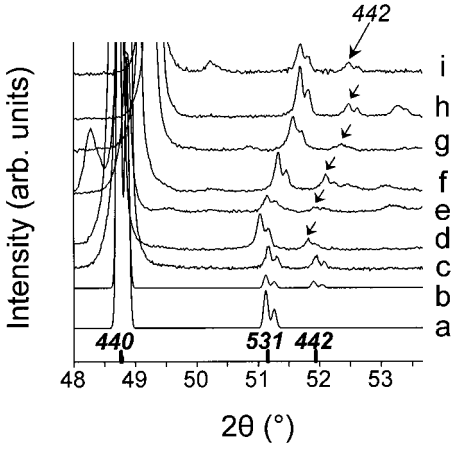

Figure 5. Selected regions of X-ray powder diffraction patterns showing that pyrochlore phases in the Bi–M–Nb–O systems (M = Zn, Co, Fe, Ni, Mn, Cu, and Cr) all exhibit weak peaks at the positions of the 442 reflections, diagnostic for displacive disorder in the A_2O' network. Patterns a) and b) are calculated for $Bi_{1.5}Zn_{0.92}Nb_{1.5}O_{6.92}$ assuming the ideal (a) pyrochlore structure (shown in part **a** of Figure 2), and (b) using the refinement results with static disordered displacements in the A and O′ sites[42] (see part **b** of Figure 2); the latter calculated pattern matches the experimentally observed pattern for $Bi_{1.5}Zn_{0.92}Nb_{1.5}O_{6.92}$ (c). The 442 reflection occurs just below 52° 2θ for the Zn compound and is forbidden in the ideal pyrochlore structure (a). This reflection is seen in all of the other patterns (at slightly shifted 2θ-values reflecting different unit cell volumes) for equilibrated specimens with nominal compositions (d) $Bi_2Co_{2/3}Nb_{4/3}O_7$, (e) $Bi_2Ni_{2/3}Nb_{4/3}O_7$, (f) Bi_2FeNbO_7, (g) Bi_2MnNbO_7, (h) $Bi_2Cu_{2/3}Nb_{4/3}O_7$, and (i) $Bi_{4/3}CrNbO_6$. Although pyrochlore is the major phase in these specimens, it does not form as a single phase at these conventional formulations.

of the cubic pyrochlore structures; the Ti^{4+} ions in the A_2O' network were displaced 0.7 Å from the ideal A sites, resulting in chemically reasonable bond lengths to five oxygen atoms, while Ca^{2+} ions remained in the ideal positions. Interestingly, the $Ca_{1.5}Ti_{1.5}NbO_7$ pyrochlore was found to exhibit dielectric relaxation similar to that of $Bi_{1.5}Zn_{0.92}Nb_{1.5}O_{6.92}$,[47] suggesting that displacive disorder, not the presence of Bi^{3+}, gives rise to this phenomenon.

Conclusions

Realizing that the pyrochlore structure can accommodate small B-type metals on up to 25% of the large A-sites by displacive disorder, solid state chemists are no longer restricted to the formula $A_2B_2O_6O'$ in the preparation of pyrochlore-type compounds with yet unknown, potentially useful properties. Many compounds can now be synthesized and/or modified by deliberate combinations of large and small metal ions on the A-sites. Since large A cations and smaller B-type cations tend to be electronically dissimilar, electrical and magnetic properties should be strongly affected by mixing them in the A_2O' network.[14] Ionic conductivity properties should also depend strongly on the occurrence of B cations, vacancies, and displacive disorder in the A_2O' network. For the theoretical community, the challenge remains to understand why some chemical systems *only* form so-called misplaced-displacive cubic pyrochlore phases, even though conventional crystal chemistry suggests that normal pyrochlores should form.

Experimental Section

Approximately 80 polycrystalline specimens (3–4 g each) were prepared in air by solid-state reactions using Bi_2O_3 (99.999%), ZnO (99.99%), and Nb_2O_5 (99.999%). Prior to each heating, each sample was mixed by grinding with an agate mortar and pestle for 15 min, pelletized, and placed on sacrificial powder of the same composition on Pt foil supported by alumina ceramic. After an initial overnight calcine at 800 °C (below the m.p. of Bi_2O_3, 825 °C) multiple 4-hour heatings (with intermediate grinding and re-pelletizing) were carried out at 950–980 °C. (Exceptions were low-melting specimens with Bi contents above 90 mol-% $BiO_{1.5}$, which were not heated above 700 °C). Samples were furnace-cooled to ca. 700 °C and then air-quenched on the bench-top. Typically, three to five heatings were required to attain equilibrium, which was presumed when no further changes could be detected in the weakest peaks observed in the X-ray powder diffraction patterns. Thermogravimetric analyses (TGA) of pure ZnO and Bi_2O_3 in flowing air indicated no significant weight loss below 1000 °C for Bi_2O_3 and about 1200 °C for ZnO. For the pyrochlore phase of composition $Bi_{1.5}Zn_{0.92}Nb_{1.5}O_{6.92}$, TGA under flowing oxygen indicated congruent-like melting at ca. 1185 °C coinciding with the onset of appreciable volatility. Single pyrochlore-type crystals were easily obtained by heating $Bi_{1.5}Zn_{0.92}Nb_{1.5}O_{6.92}$ powder in a Pt capsule (sealed by welding) to 1275 °C, followed by slow-cooling (5 °C/h) to below the freezing point.

Polycrystalline pyrochlore-containing specimens in the Bi–M–Nb–O systems (M = Co, Ni, Fe, Mn, Cu, and Cr) were synthesized as above at the following chemical compositions, with reagents and final soak temperatures in parentheses: $Bi_2Co_{2/3}Nb_{4/3}O_7$ (Co_3O_4, spectroscopic grade, pre-analyzed by TGA, 925 °C), $Bi_2Ni_{2/3}Nb_{4/3}O_7$ (NiO, 99.998%, 925 °C), Bi_2FeNbO_7 (Fe_2O_3, reagent grade, 925 °C), Bi_2MnNbO_7, ($MnCO_3$, reagent grade, pre-analyzed by TGA, 885 °C), $Bi_2Cu_{2/3}Nb_{4/3}O_7$ (CuO, reagent grade, 825 °C), and $Bi_{4/3}CrNbO_6$ (Cr_2O_3, reagent grade, 975 °C). All specimens, when equilibrated, were mixtures containing pyrochlore as the major phase.

Phase assemblages in the Bi_2O_3–ZnO–Nb_2O_5 system were ascertained using the disappearing phase method[66,67] and X-ray powder diffraction data obtained with a Philips[68] diffractometer equipped with incident Soller slits, a theta-compensating slit and graphite monochromator, and a scintillation detector. Samples were mounted in welled glass slides. Patterns were collected at ambient temperatures using Cu-K_α radiation over the range 3–70° 2θ with a 0.02° 2θ step size and a 2 s count time. Intensity data measured as relative peak heights above background were obtained using the DATASCAN software package, and processed using JADE. For unit cell refinements, observed 2θ line positions were first corrected using SRM 660, LaB_6,[69] as an external calibrant. Lattice parameters were refined using JADE (2θ values, Cu-$K_{\alpha1}$ = 1.540593 Å).

Unit cell parameters and compositions for several single-phase pyrochlore specimens are given in Table 1. The present data suggest that the limiting compositions of the pyrochlore phase field, located at the four cusps (corners) in Figure 4, are approximately $Bi_{1.64}Zn_{0.33}(Zn_{0.52}Nb_{1.48})O_7$ (highest Bi-content), $Bi_{1.61}Zn_{0.39}(Zn_{0.55}Nb_{1.46})O_7$, $Bi_{1.48}Zn_{0.44}(Zn_{0.44}Nb_{1.56})O_7$ (highest Nb-content), and $Bi_{1.47}Zn_{0.52}(Zn_{0.48}Nb_{1.52})O_7$ (lowest Bi-content,

highest Zn-content). During synthesis, the pyrochlore phase formed early in partially reacted samples and was readily purified within the single-phase region, suggesting high thermodynamic stability.

Table 1. Compositions, cubic unit cell parameters (***a***, space group $Fd\bar{3}m$, #227), and structural formulas for single-phase pyrochlore specimens. These compositions correspond to the points within the four-sided pyrochlore region shown in Figure 4. The structural formulas have been normalized to seven oxygen atoms (full occupancy of the O′ site) for purposes of comparison. Parentheses denote cations in the octahedral B-sites.

Composition	*A* [Å]	Structural formula
$Bi_{1.50}Zn_{0.91}Nb_{1.54}O_7$	10.551(1)	$Bi_{1.50}Zn_{0.45}(Zn_{0.46}Nb_{1.54})O_7$
$Bi_{1.52}Zn_{0.93}Nb_{1.52}O_7$	10.555(1)	$Bi_{1.50}Zn_{0.45}(Zn_{0.48}Nb_{1.52})O_7$
$Bi_{1.55}Zn_{0.91}Nb_{1.51}O_7$	10.553(1)	$Bi_{1.55}Zn_{0.42}(Zn_{0.49}Nb_{1.51})O_7$
$Bi_{1.60}Zn_{0.93}Nb_{1.47}O_7$	10.564(1)	$Bi_{1.60}Zn_{0.40}(Zn_{0.53}Nb_{1.47})O_7$
$Bi_{1.63}Zn_{0.88}Nb_{1.47}O_7$	10.571(1)	$Bi_{1.63}Zn_{0.35}(Zn_{0.53}Nb_{1.47})O_7$

Acknowledgments

We thank R. S. Roth for helpful discussions, L. P. Cook for thermogravimetric analyses, J. Suh for technical assistance, and P. K. Schenk and N. Swanson for graphical representation of the phase diagram data.

[1] R. V. Gaines, H. C. W. Skinner, E. E. Foord, B. Mason, A. Rosenzweig (Eds.), *Dana's New Mineralogy*, Wiley: New York, **1997**, pp. 341–352, 8th edition.
[2] So diverse that geologists have referred to the pyrochlore structure as a "chemical garbage can".
[3] A *Web of Science* search (1975 to present) for articles containing the term *pyrochlore* in the title returned 837 hits.
[4] M. A. Subramanian, G. Aravamudan, G. V. Subba Rao, *Prog. Solid State Chem.* **1983**, *15*, 55 an extensive pyrochlore review covering literature up to ca. 1981.
[5] B. J. Kennedy, *Physica B* **1998**, *241–243*, 303.
[6] L. Minervini, R. W. Grimes, *J. Am. Ceram. Soc.* **2000**, *83*, 1873, and references therein.
[7] B. J. Wuensch, K. W. Eberman, C. Heremans, E. M. Ku, P. Onnerud, E. M. E. Yeo, S. M. Haile, J. K. Stalick, J. D. Jorgensen, *Solid State Ionics* **2000**, *129*, 111.
[8] M. Pirzada, R. W. Grimes, J. F. Maguire, *Solid State Ionics* **2003**, *161*, 81, and references therein.
[9] G. D. Blundred, C. A. Bridges, M. J. Rosseinsky, *Angew. Chem. Int. Ed.* **2004**, *43*, 3562, and references therein.
[10] G. Jeanne, G. Desgardin, G. Allais, B. Raveau, *J. Solid State Chem.* **1975**, *15*, 193, and references therein.
[11] D. Bernard, J. Pannetier, J. Lucas, *Ferroelectrics* **1978**, *21*, 429.
[12] C. A. Randall, J. C. Nino, A. Baker, H.-J. Youn, A. Hitomi, R. Thayer, L. F. Edge, T. Sogabe, D. Anderson, T. R. Shrout, S. Trolier-McKinstry, M. Lanagan, *Bull. Am. Ceram. Soc.* **2003**, *82*, 9101, and references therein.
[13] R. J. Cava, W. F. Peck, J. J. Krajewski, *J. Appl. Phys.* **1995**, *78*, 7231, and references therein.
[14] M. Avdeev, M. K. Haas, J. D. Jorgensen, R. J. Cava, *J. Solid State Chem.* **2002**, *169*, 24.
[15] S. Yonezawa, Y. Muraoka, Y. Matsushita, Z. Hiroi, *J. Phys. Soc. Japan* **2004**, *73*, 819.
[16] E. Beck, A. Ehmann, B. Krutzsch, S. Kemmler-Sack, H. R. Khan, C. J. Raub, *J. Less-Common Met.* **1989**, *147*, L17.
[17] G. Mayer-Von Kuerthy, W. Wischert, R. Kiemel, S. Kemmler-Sack, *J. Solid State Chem.* **1989**, *79*, 34.
[18] L. Li, B. J. Kennedy, *Chem. Mater.* **2003**, *15*, 4060, and references therein.
[19] A. P. Ramirez, A. P. Hayashi, A. R. J. Cava, R. Siddharthan, B. S. Shastry, *Nature* **1999**, *399*, 333.
[20] J. E. Greedan, J. Avelar, M. A. Subramanian, *Solid State Commun.* **1992**, *82*, 797, and references therein.
[21] M. A. Subramanian, C. C. Torardi, D. C. Johnson, J. Pannetier, A. W. Sleight, *J. Solid State Chem.* **1988**, *72*, 24.
[22] Y. Shimakawa, Y. Kubo, T. Manako, *Nature* **1996**, *379*, 53.
[23] M. A. Subramanian, B. H. Toby, A. P. Ramirez, W. J. Marshall, A. W. Sleight, G. H. Kwei, *Science* **1996**, *273*, 81.
[24] M. Hamoumi, M. Wiegel, G. Blasse, *J. Solid State Chem.* **1994**, *108*, 410.
[25] R. C. Ewing, W. J. Weber, J. Lian, *J. Appl. Physics* **2004**, *95*, 5949, an extensive review.
[26] A. F. Wells, *Structural Inorganic Chemistry*, Clarendon: Oxford, **1975**, pp. 209, 499, 4th edition.
[27] B. G. Hyde, S. Andersson, *Inorganic Crystal Structures*, Wiley: New York, **1989**, pp. 344–349.
[28] The prefix "*anti-*" refers to switching of the cation and anion positions. Compared to the β-cristobalite (SiO_2) structure, the A cations occupy the oxygen positions and the O′ oxygen atoms occupy the Si positions.
[29] R. Nedjar, M. M. Borel, M. Hervieu, B. Raveau, *Mater. Res. Bull.* **1988**, *23*, 91.
[30] J. Miranday, G. Gauthier, R. DePape, *C. R. Acad. Sci., Ser. B* **1971**, *273*, 970.
[31] D. Bernard, J. Pannetier, J. Y. Moisan, J. Lucas, *J. Solid State Chem.* **1973**, *8*, 31.
[32] H. Nyman, S. Andersson, B. G. Hyde, M. O'Keeffe, *J. Solid State Chem.* **1978**, *26*, 123.
[33] M. Ledesert, B. Raveau, *J. Solid State Chem.* **1987**, *67*, 340.
[34] N. Ruchard, J. Grannec, A. Tressaud, P. Gravereau, *C. R. Acad. Sci. II, Ser. B* **1995**, *321*, 507.
[35] Y. Calage, M. Zemirli, J. M. Greneche, F. Varret, R. DePape, G. Ferey, *J. Solid State Chem.* **1987**, *69*, 197.
[36] O. Muller, R. Roy, *The Major Ternary Structural Families*, Springer-Verlag: New York, **1974**, pp. 4–14.
[37] As determined from observed bond lengths, values are from R. D. Shannon, *Acta Crystallogr., Sect. B* **1976**, *32*, 751.
[38] R. S. Roth, *J. Res. NBS* **1956**, *56*, 17.
[39] E. Aleshin, R. Roy, *J. Am. Ceram. Soc.* **1962**, *45*, 18.
[40] B. C. Chakoumakos, *J. Solid State Chem.* **1984**, *53*, 120.
[41] N. Wakiya, A. Saiki, N. Kieda, K. Shinozaki, N. Mizutani, *J. Solid State Chem.* **1992**, *101*, 71.
[42] V. S. Darshane, *J. Indian Chem. Soc.* **1980**, *57*, 108.
[43] M. Valant, P. K. Davies, *J. Am. Ceram. Soc.* **2000**, *83*, 147, and references therein.
[44] I. Levin, T. G. Amos, J. C. Nino, T. A. Vanderah, C. A. Randall, M. T. Lanagan, *J. Solid State Chem.* **2002**, *168*, 69.
[45] R. L. Withers, T. R. Welberry, A.-K. Larsson, Y. Liu, L. Norén, H. Rundlöf, F. J. Brink, *J. Solid State Chem.* **2004**, *177*, 231.
[46] W. G. Mumme, I. E. Grey, R. S. Roth, personal communication (with permission) that the model was refined to an *R* factor of 4%.
[47] S. Kamba, V. Porokhonskyy, A. Pashkin, V. Bovtun, J. Petzelt, J. C. Nino, S. Trolier-McKinstry, M. T. Lanagan, C. A. Randall, *Phys. Rev. B* **2002**, *66*, 54106.
[48] R. S. Roth, J. L. Waring, *J. Res. NBS* **1962**, *66A*, 451.
[49] C. D. Ling, R. L. Withers, S. Schmid, J. G. Thompson, *J. Solid State Chem.* **1998**, *137*, 42.
[50] M. Valant, D. Suvorov, *J. Am. Ceram. Soc.* **2003**, *86*, 939.
[51] J. P. Guha, S. Kunej, D. Suvorov, *J. Mater. Sci.* **2004**, *39*, 911.
[52] A. A. Ballman, H. Brown, *J. Cryst. Growth* **1977**, *41*, 36.
[53] R. R. Dayal, *J. Less-Common Met.* **1972**, *26*, 381.
[54] I. Levin, T. G. Amos, J. C. Nino, T. A. Vanderah, I. M. Reaney, C. A. Randall, M. T. Lanagan, *J. Mater. Res.* **2002**, *17*, 1406.
[55] The zirconolite and pyrochlore structures are related but distinctly different. In zirconolite-type $Bi_2Zn_{2/3}Nb_{4/3}O_7$, Zn^{2+} ions are also displacively disordered near the centers of six-membered rings of $[(Nb,Zn)O_6]$ octahedra, resulting in a (5 + 1) co-

ordination environment similar to that of the A-site Zn^{2+} ions in pyrochlore-type $Bi_{1.5}Zn_{0.92}Nb_{1.5}O_{6.92}$[42].
[56] T. Birchall, A. W. Sleight, *J. Solid State Chem.* **1975**, *13*, 118.
[57] I. Radosavljevic, J. S. O. Evans, A. W. Sleight, *J. Solid State Chem.* **1998**, *136*, 63.
[58] A. L. Hector, S. B. Wiggin, *J. Solid State Chem.* **2004**, *177*, 139, and references therein.
[59] S. Uma, S. Kodialam, A. Yokochi, N. Khosrovani, M. A. Subramanian, A. W. Sleight, *J. Solid State Chem.* **2000**, *155*, 225, and references therein.
[60] Y. Tabira, R. L. Withers, T. Yamada, N. Ishizawa, *Z. Kristallogr.* **2001**, *216*, 92, and references therein.
[61] V. P. Sirotinkin, A. A. Bush, *Inorg. Materials* **2003**, *39*, 974.
[62] I. Pazos, A. Adler, M. Lufaso, T. Vanderah, results presented at the Summer Undergraduate Research Fellowship Symposium, National Institute of Standards and Technology, Gaithersburg, MD, August 10–11, **2004**, manuscripts in preparation.
[63] U. Ismunandar, T. Kamiyama, K. Oikawa, A. Hoshikawa, B. J. Kennedy, Y. Kubota, K. Kato, *Mater. Res. Bull.* **2004**, *39*, 553.
[64] A. Jongejan, A. L. Wilkins, *J. Less-Common Met.* **1970**, *21*, 225.
[65] P. Bordet, L. Cranswick, W. G. Mumme, R. S. Roth, I. E. Grey, (with permission), manuscript in preparation.
[66] C. G. Bergeron, S. H. Risbud, *Introduction to Phase Equilibria in Ceramics*, American Ceramic Society: Westerville, **1984**.
[67] C. S. Barrett, *Structure of Metals*, McGraw-Hill: New York, **1943**, chapter X, 1st edition.
[68] Certain commercial equipment and software are identified in order to adequately specify the experimental procedure; recommendation or endorsement by the National Institute of Standards and Technology is not therein implied.
[69] C. R. Hubbard, Y. Zhang, R. L. McKenzie, *Certificate of Analysis, SRM 660*, National Institute of Standards and Technology, Gaithersburg, MD, 20899, **1989**.

Received: March 18, 2005
Published Online: June 17, 2005

